Generating Ambiguous Figure-Ground Images

Ying-Miao Kuo, Hung-Kuo Chu, Ming-Te Chi, Ruen-Rone Lee, and Tong-Yee Lee, *Senior Member, IEEE*

Abstract—Ambiguous figure-ground images, mostly represented as binary images, are fascinating as they present viewers a visual phenomena of perceiving multiple interpretations from a single image. In one possible interpretation, the white region is seen as a foreground figure while the black region is treated as shapeless background. Such perception can reverse instantly at any moment. In this paper, we investigate the theory behind this ambiguous perception and present an automatic algorithm to generate such images. We model the problem as a binary image composition using two object contours and approach it through a three-stage pipeline. The algorithm first performs a partial shape matching to find a good partial contour matching between objects. This matching is based on a content-aware shape matching metric, which captures features of ambiguous figure-ground images. Then we combine matched contours into a compound contour using an adaptive contour deformation, followed by computing an optimal cropping window and image binarization for the compound contour that maximize the completeness of object contours in the final composition. We have tested our system using a wide range of input objects and generated a large number of convincing examples with or without user guidance. The efficiency of our system and quality of results are verified through an extensive experimental study.

Index Terms—Figure-ground perception, partial shape matching, curve deformation, image cropping, image binarization

1 Introduction

Ambiguous figure-ground perception, also referred as figure-ground reversal, is a visual phenomenon where the perception of a meaningful object, the *figure*, and a shapeless background, the *ground*, is not constant in an image, and can reverse spontaneously [1]. The best known example illustrating such a particular perceptual experience is probably the Face-Vase illusion drawn by Edgar Rubin as shown in Fig. 1. In this image the viewer can perceive either the central white region or the surrounding black region as the figure at any moment. In the former, the contour of the white region defines the shape of a vase while the opposite black region is regarded as the background. Such assignment of figure and ground is instantly reversed when the black region is interpreted as a figure depicting two face-to-face human profiles.

The unique mental skill of humans to spontaneously reverse figure-ground perception is closely related to a fundamental component in perceptual organization, namely *figure assignment*. It has been well studied in Gestalt psychology that the inhibitory competition between cues along the opposite sides of a boundary shared by two contiguous regions in the visual field plays an important role in the figure assignment process [2], [3], [4], [5], [6]. Both the low-level geometric features (e.g., convexity, symmetry, enclosure, etc) and high-level cues (e.g., attention, familiarity, past experience, etc) are reported to affect the competition process [3], [7], [8], [9]. The figure is perceived on the side that wins the competition while the opposite region is perceived as shapeless ground. This suggests a mechanism to create an effective ambiguous figure-ground image by combining two objects in a form where the competition of figure assignment is evenly matched along the shared boundary.

As an art form, ambiguous figure-ground images are fascinating to look at and widely used in advertising designs [10]. To create effective and aesthetic art pieces, the artist and designer strike a delicate balance in keeping salient features of two tightly interlocked objects along the shared boundary. The creation process may involve tedious trial-and-error runs to place two objects in a proper spatial configuration (i.e., position, orientation, and scale) and determine a shared boundary between two objects. Then adjoined regions need to be filled up with contrast colors (e.g., black and white) to differentiate between figure and ground regions in the final composition. Thus manually creating such images is challenging even for a skilled designer. In this work, we design computational tools to facilitate such a process.

However, designing a computational model for generating effective and visually appealing ambiguous figure-ground images that does not require the kinds of skills employed by artists poses the main challenge. Inspired by the representation of art works, we model the problem as finding a binary image composition of two objects such that the outlines of black and white regions effectively delineate the shapes of objects. We approach the problem using a novel three-stage algorithm, involving shape matching and deformation to compute and stitch two objects at partial matching contours, followed by image cropping and binarization to get the final composition. In the key *partial shape matching* stage, we propose a novel content-aware shape matching metric for evaluating the quality of partial contour

- *Y.-M. Kuo, H.-K. Chu, and R.-R. Lee are with the Computer Science, National Tsing Hua University, Hsinchu 30013, Taiwan. E-mail: jollytreeskuo@gmail.com, {hkchu, rrlee}@cs.nthu.edu.tw.*
- *M.-T. Chi is with the Computer Science, National Chengchi University, Taipei, Taiwan. E-mail: mtchi@cs.nccu.edu.tw.*
- *T.-Y. Lee is with the Computer Science and Information Engineering, National Cheng-Kung University, Tainan, Taiwan. E-mail: tonylee@mail.ncku.edu.tw.*

Manuscript received 12 May 2015; revised 6 Feb. 2016; accepted 11 Feb. 2016. Date of publication 26 Feb. 2016; date of current version 29 Mar. 2017. Recommended for acceptance by T. Ju. For information on obtaining reprints of this article, please send e-mail to: reprints@ieee.org, and reference the Digital Object Identifier below. Digital Object Identifier no. 10.1109/TVCG.2016.2535331

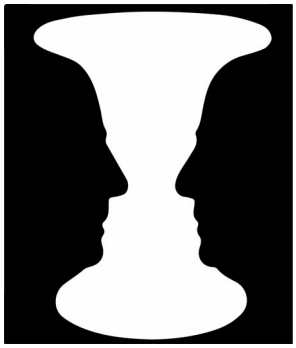

Fig. 1. A classic example of ambiguous figure-ground image. The perception of a white vase on a black background or two black human profiles in front of a white background can exchange spontaneously.

matching based on the measurable convexity cue in inhibitory competition theory. The metric measures not only (i) the conventional local shape similarity, but also captures features to render ambiguous figure-ground images, including (ii) how well the convexity cues of objects are retained along the matching contours; (iii) the length of matching contours; (iv) how much deformation is required to merge two matching contours into a common boundary; and (v) the orientation of objects. In other words, the system prefers two objects to match with each other in the familiar upright orientation and at longer partial contours where the convex parts of an object precisely match the concave parts of the others and vice versa. Then we perform a *contour deformation* to merge two matched partial contours into a common boundary and obtain a compound contour. The last stage aims to compute an optimal window frame enclosing the compound contour and binary color assignment of pixels to form the final binary image. This is done by a joint optimization that simultaneously computes *image cropping* and *binarization* to maximize the completeness of original object contours in the composition. To the best of our knowledge, our system is the first one that presents a computational model to automatically generate ambiguous figure-ground images.

Although our algorithm runs automatically, the system offers additional user interfaces to allow both amateur and advanced users to intervene in the creation process. Specifically, users can optionally select partial contours of input objects to guide the partial shape matching process. The system generates multiple matching hypotheses ranked by the estimated shape matching cost, while users are able to select among them the one they find interesting. Users can further override the suggested cropping window by specifying a new one, while the system, in the background, automatically updates the binary image. Please see the supplementary video, which can be found on the Computer Society Digital Library at http://doi.ieeecomputersociety.org/10.1109/TVCG.2016.2535331, for such a user session.

We have tested our system using a wide range of input objects and generated a large number of convincing examples (60 images) with or without user guidance. The effectiveness of perceiving figure-ground reversal in our results is verified by a user study. The results indicate that our system is efficient and flexible for users to interactively create ambiguous figure-ground images. Fig. 2 shows an example generated using our system.

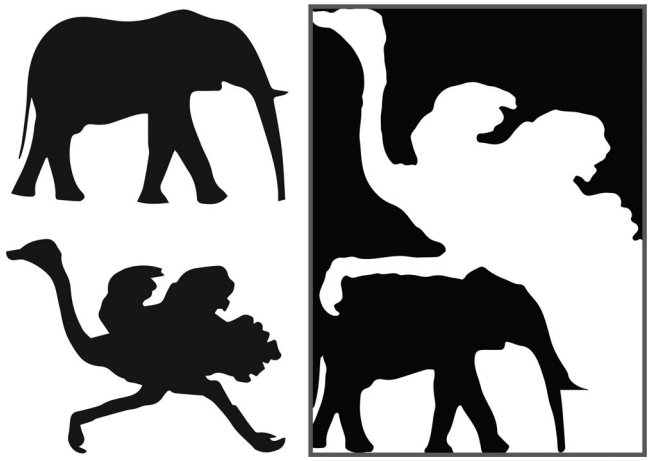

Fig. 2. An ambiguous figure-ground image created by our system. The input objects are shown on the left.

Contributions. In summary, our contributions include:

- an interactive system that facilitates creating effective and appealing ambiguous figure-ground images;
- investigating the guiding principles behind the ambiguous figure-ground perception, based on which we develop computational models to tackle the composition problem;
- a novel partial shape matching based on a content-aware shape matching metric that is capable of measuring multiple matching criteria and tailored to capture characteristics of ambiguous figure-ground images; and
- a joint optimization that simultaneously computes optimal image cropping and binarization to maximize the completeness of object contours in the final composition.

2 Related Work

2.1 Perceptual Organization

The ability to perceive ambiguous figure-ground reversal is closely related to a fundamental operation in perceptual organization, figure assignment, which distinguishes meaningful figure from shapeless ground from two contiguous regions. It has been extensively studied in psychological research about what kind of factors influence figure assignment. In the classic point of view, the figure assignment is believed to occur at a low-level in the visual hierarchy and is affected only by geometric features [7], [9], [11]. The empirical studies demonstrate that viewers tend to perceive regions that are convex, symmetric or enclosed as figures rather than those are concave, asymmetric or enclosing. The modern theoretic models of figure-ground perception further introduce high level factors, such as attention, familiarity and past experience [2], [3], and assume an inhibitory competition between both low-level and high-level cues [2], [4], [5]. We refer the reader to [6] for a comprehensive survey. Our method is mainly inspired by the inhibitory competition model and aims at finding a binary image composition where the figural competition of two objects in convexity cue is evenly matched along the shared boundaries.

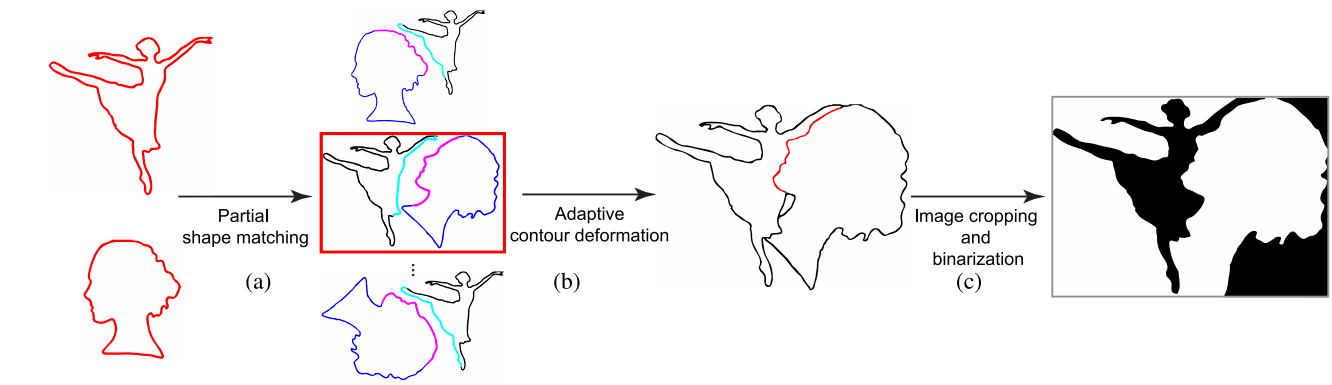

Fig. 3. An overview of our system to automatically generate an ambiguous figure-ground image using two outer contours extracted from input images. (a) The system starts by finding candidate partial contour matches based on a novel content-aware shape matching metric. (b) The matching pair with top score is selected by the system and both matched contours are adaptively deformed to share a common boundary. (c) Last, the system computes an optimal cropping window and image binarization to maximize the completeness of object contours in the final result.

2.2 Computational Arts

Computer aided design of recreational arts has been an active research topic in computer graphics in the recent decade. Previous researches that are related to our topic appear in various contexts including illusory art [12], [13], hidden images [14], [15], [16], [17], and collage art [18], [19], [20], [21], etc. Among the diverse and vast existing researches, our method bears partial similarity to works based on shape matching [15], [18], [19], [20], [21]. Kaplan and Salesin [18] propose a solution to the 'Escherization' problem that finds a regular tiling using a closed figure resembling the original input image. Gal et al. [19] design a 3D collage system that mimics Acrimboldo's paintings by assembling common 3D shapes to form a compound object. The idea is later reformulated by Huang et al. [20] who utilize internet images to compose a 2D figure that resembles the input image. Yoon et al. [15] present a hidden-picture puzzle generator that aims at finding suitable places to hide small objects in a cluttered background image. Tong et al. [21] present an automatic system for creating nested images. The system embeds an inner figure within an outer figure based on a contour matching that considers the holes of former figure and the contour of latter one. While these works successfully generate impressive results, their previous systems are customized for generating specific art forms, which are fundamentally different from ambiguous figure-ground images. Thus, none of these previous approaches can be directly used to solve our problem of compositing a binary image from two objects.

2.3 Shape Matching

Shape matching is a well-studied topic in computer vision and can be roughly divided into two categories, the brightness- and feature-based methods [22]. The brightness-based approaches treat the intensity of each pixel as the shape descriptor, which is sensitive to the changes in object poses and image illumination [23]. In contrast, feature-based approaches [24], [25], [26], [27], [28] describe the shapes of objects using geometric properties of the image (e.g., contours, sample points, etc), and are proved to obtain better performance. For instance, Belongie et al. [25] efficiently perform global shape matching based on the translate- and scale-invariant shape context descriptors. However, the global shape matching is fragile to images with strong articulation and occlusion. To address the problem, Donoser et al. [27] introduce a novel chord angle descriptor that encodes both local and global information and is invariant to similarity transformations. An integral image based shape matching, namely IS-Match, is presented to efficiently return a large set of partial sub-matches. The IS-Match algorithm is further extended by Riemenschneider et al. [28] to handle objects with open contours. However, such conventional shape matching algorithms, which measure only the shape similarity between objects, frequently fail to generate promising ambiguous figure-ground images (see Section 8.3). In this work, we propose a novel shape matching with a content-aware shape metric tailored for capturing dominant characteristics that render effective ambiguous figure-ground images.

3 Overview

An overview of our system is shown in Fig. 3. The system takes two object images as inputs and extracts the outer contours to serve as the basic processing units. Such contour images can be generated from clip arts or converted from raster images using image filtering such as artistic thresholding [29]. The system starts by finding partial contour matches between two objects based on a content-aware shape matching metric. This metric is tailored to capture features of ambiguous figure-ground images and measures the local shape similarity, the lengths of the matching contours, the matching degree in convexity cues, the global shape deformation energy, and the object orientation (see Section 4.1). Specifically, we first perform an efficient partial shape matching algorithm to obtain a large set of sub-matching contours based on local shape similarity (see Section 4.2). These sub-matching contours are further clustered based on the similarity of pairwise rigid transformation estimated using the matching contour points (see Section 4.3). For each cluster, we compute an optimal partial contour matching along with a sequence of matching contour points by integrating the constituent sub-matching contours. This is done by solving a minimum weighted bipartite matching of a graph where the edge weight captures the local shape similarity, the matching degree in convexity cues and the shape deformation between matching contour points (see Section 4.4). Clusters are ranked according to the evaluated shape matching cost, and the system selects the top 5 as candidate shape matching pairs.

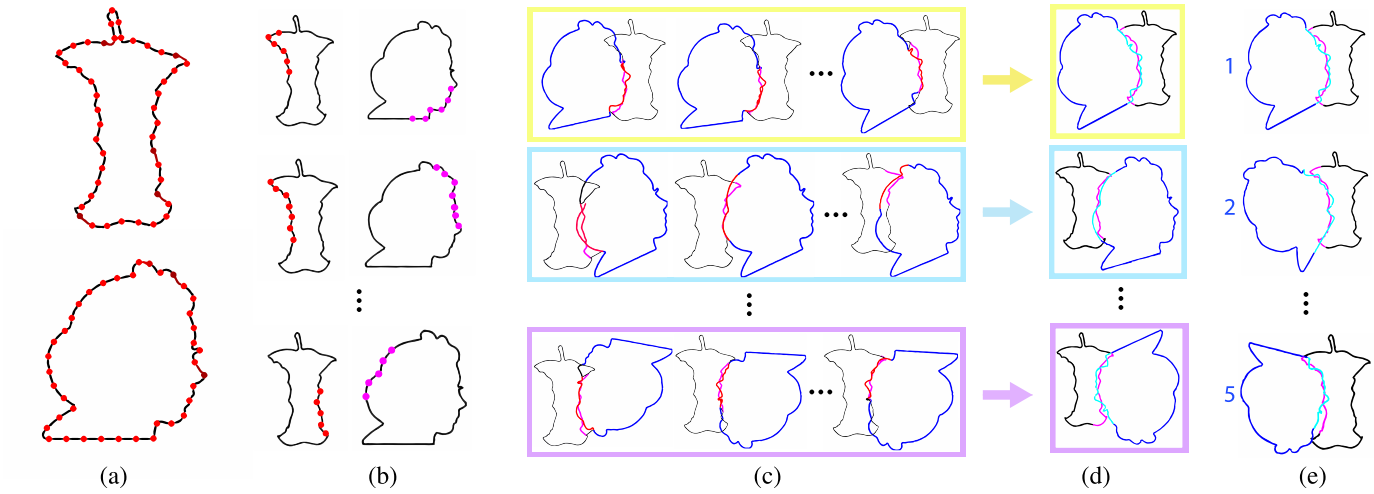

Fig. 4. Partial shape matching pipeline. (a) The input contours and sampled points. (b) Initial sub-matching contours returned by the IS-Match. (c) Grouping the sub-matching pairs with similar rigid transformations into clusters. (d) Estimating an optimal partial contour matching for each cluster. (e) The candidate partial shape matching results with top five scores.

Given a shape matching pair, the system combines two objects to share a common boundary by deforming the corresponding matching contours. The contour deformation is guided by the measured convexity on the matching contour points, and an as-rigid-as possible shape deformation is employed to obtain a smooth result (see Section 5). To generate the final binary image composition, the system determines a cropping window and renders the cropped image using black and white to distinguish figure and ground regions. We propose a joint optimization that iteratively adjusts the dimensions of the cropping window and computes the image binarization to maximize the completeness of object contours (see Section 6). Our system is flexible and offers intuitive user controls. Users are able to go back and forth between the above processes, override the suggestions made by the system, and explore the creation in different dimensions (see Section 7).

4 Partial Shape Matching

Given two input objects and corresponding outer contours, the key step toward generating an effective ambiguous figure-ground image is to find a good partial shape matching between two contours. While a major effort from researchers has been devoted to designing shape descriptors that measure local shape similarity, we propose a novel partial shape matching algorithm with a tailor-made metric that measures multiple matching criteria. Specifically, we design a *content-aware shape matching metric* to find partial contour matches where (i) the local shapes of matching contours are similar; (ii) the convex parts of a particular contour match the concave parts of the other one and vice versa; (iii) the length of matching contours is as long as possible; (iv) the shape deformation required to merge two matching contours into a common boundary is minimum; and (v) objects are matched in their upright orientation. While the first criterion inherits the conventional setting, the other four criteria are mainly inspired by the theoretic model and artistic works that render effective and visually appealing ambiguous figure-ground images.

4.1 Content-Aware Shape Matching Metric

We denote two outer contours as $C_a = \{a_i | i = 1, \ldots, n_a\}$ and $C_b = \{b_j | j = 1, \ldots, n_b\}$, where $a_i, b_j \in \mathbb{R}^2$ represent the ordered sampling points on both contours, respectively (see Fig. 4a). A partial shape matching is represented as $\{c_a, c_b, \pi, \mathbf{T}\}$, indicating two partial contours, $c_a \in C_a$ and $c_b \in C_b$, are matched on a sequence of order-preserved matching points $\{(a_i, b_{\pi(i)}) | a_i \in c_a, b_{\pi(i)} \in c_b\}$, where π is a bijective function and $\mathbf{T} = (d_x, d_y, \theta)$ is a 2D rigid transformation that maps the c_a onto c_b with a displacement (d_x, d_y) and planar rotation of angle $\theta \in [-180°, 180°]$. We estimate $\mathbf{T}$ by minimizing the following objective function:

$$E = \sum_{\forall a_i \in c_a} \|\mathbf{T}(a_i - \bar{a}) - b_{\pi(i)}\|^2, \tag{1}$$

where $\bar{a}$ is the centroid of the C_a. Equation (1) is solved using SVD and we employ the RANSAC algorithm to improve robustness. Now let us define the matching metrics as follows:

Shape similarity cost. This metric aims at capturing the local shape similarity between matching contours. We adopt the chord angle shape descriptor introduced by Donoser et al. [27] to encode a descriptor matrix for each object contour and denote them as $\mathbf{M}_a$ and $\mathbf{M}_b$. The distance between two partial contours is defined as:

$$E_s(c_a, c_b, \pi) = \frac{1}{N_\pi^2} \sum_{i=s}^{i<s+N_\pi} \sum_{j=s}^{j<s+N_\pi} [\mathbf{M}_a(i, j) - \mathbf{M}_b(\pi(i), \pi(j))]^2, \tag{2}$$

where N_π represents the number of pairs of matching points and s is the index of the first sampling point of c_a in C_a. We refer the reader to [27] for more details about the definition of Equation (2). Note that while there are other alternatives, we favor the chord angle descriptor because it is invariant to similarity transformations.

Convexity matching cost. This metric is used to measure how well the convex parts of c_a match the concave parts of c_b and vice versa. To quantify the convexity cue on a contour, we first apply the Douglas-Peucker algorithm [30] to approximate a curve contour using a polyline with the

vertices $\{v_1, \ldots, v_n\}$ in counter-clockwise order. The magnitude of the convexity cue at each vertex is defined as:

$$\alpha(v_i) = \mathrm{sgn}((v_i - v_{i-1}) \times (v_{i+1} - v_i)) \cdot \frac{|\angle v_{i-1} v_i v_{i+1} - 180|}{180},$$

where the $\mathrm{sgn}(\cdot)$ represents a sign function and $\angle v_{i-1} v_i v_{i+1}$ is the internal angle of v_i. The range of $\alpha(\cdot)$ is $[-1.0, 1.0]$, where the positive and negative value represent respectively the convex and concave vertices. The larger (smaller) the value, the higher the degree of convexity (concavity) is at the vertex. The magnitude of the convexity cue at contour points is computed by modulating the value of nearest vertex by a Gaussian function. The cost function is then defined as:

$$\begin{aligned} E_c(c_a, c_b, \pi) &= 1.0 + \frac{1}{N_\pi} \sum_{\forall a_i \in c_a} f_c(a_i, b_{\pi(i)}), \\ f_c(a_i, b_{\pi(i)}) &= \mathrm{sgn}(\alpha_a(a_i) \cdot \alpha_b(b_{\pi(i)})) \cdot \sqrt{|\alpha_a(a_i) \cdot \alpha_b(b_{\pi(i)})|}. \end{aligned} \tag{3}$$

Note that a smaller value indicates a better matching result.

Matching length cost. The cost function prefers a partial contour matching that takes a large portion of input contours and is defined as:

$$E_l(c_a, c_b, \pi) = 1.0 - \max\left\{\frac{\|c_a\|}{\|C_a\|}, \frac{\|c_b\|}{\|C_b\|}\right\}, \tag{4}$$

where the term $\frac{\|c_i\|}{\|C_i\|}$ indicates the ratio of length of the partial contour c_i to that of original contour C_i.

Shape deformation cost. Since we need to determine a composition where two objects are combined and partially share a common boundary, we measure in advance how much shape deformation is expected to merge two matching contours, ca and cb, into a common boundary. Specifically, this cost function computes the average displacement between matching points after the contour c_a is mapped onto c_b through the optimal rigid transformation $\mathbf{T}$, and is defined as:

$$\begin{aligned} E_d(c_a, c_b, \pi, \mathbf{T}) &= \frac{1}{N_\pi} \sum_{\forall a_i \in c_a} f_d(a_i, b_{\pi(i)}, \mathbf{T}), \\ f_d(a_i, b_{\pi(i)}, \mathbf{T}) &= \|\mathbf{T}(a_i - \bar{a}) - b_{\pi(i)}\|. \end{aligned} \tag{5}$$

A better matching indicates a smaller amount of deformation, which is required in the latter contour deformation stage.

Shape orientation cost. The experimental studies reported by Peterson and Gibson [3] indicate that an object is more likely to be perceived as figure when it is presented in its upright orientation rather than in an inverted setting. Hence we model this particular perceptual feature by penalizing the shape matching where the object deviates from its upright orientation in rotation space. The cost function is thus defined as:

$$E_o(\mathbf{T}) = 1.0 - \exp\left(\frac{\theta^2}{2\sigma^2}\right), \tag{6}$$

where θ is the angle of rotation of optimal rigid transformation that maps c_a onto c_b, and we use the default setting of $\sigma = 45$.

Total matching cost. Given the definition of matching metrics, the partial shape matching problem is formulated as minimizing a total matching cost:

$$\{c_a^*, c_b^*, \pi^*, \mathbf{T}^*\} = \arg\min_{c_a, c_b, \pi, \mathbf{T}} [\omega_s E_s + \omega_c E_c + \omega_l E_l + \omega_d E_d + \omega_o E_o], \tag{7}$$

with ω_i controlling the relative importance of cost functions. Unless otherwise mentioned, we use the default parameters setting of $\omega_s = 5$, $\omega_c = 20$, $\omega_l = 60$, $\omega_d = 1$, and $\omega_o = 15$ for generating all the examples in this paper. Nevertheless, computing an optimal partial shape matching that minimizes Equation (7) is non-trivial and, to the best of our knowledge, has not been addressed by previous methods. We tackle the optimization problem using a divide-and-conquer algorithm as elaborated below.

4.2 Initial Sub-Matching Contours

The matching process is bootstrapped by finding partial contour matches that are similar in local shape. We employ an efficient partial shape matching algorithm by Donoser et al. [27], namely IS-Match, to retrieve a large set of sub-matching contours using a chord angle descriptor. To adapt to IS-Match framework, we make the following assumptions and preprocessing on input images. (i) Since the IS-Match is sensitive to the size of input images, we first resize two images to have equal diagonal length. Then we enrich the samples of input contours by resizing a particular contour (e.g., C_a) at different scales and adding mirror images to improve the likelihood of good matches. We use scaling factors ranging from 0.6 to 1.4 with an interval of 0.2 to obtain 10 different samples. For simplicity in notation, we use C_a to represent any instance of samples. (ii) In order to capture the shape orientation in Equation (6), we assume the input objects are already in their upright orientaion. (iii) The object contours are closed and the sampling points are generated with equidistant sampling to improve the robustness of partial shape matching [27]. The IS-Match outputs a set of sub-matching pairs with the matching cost below a fixed threshold. Note that while there are other alternatives, we find the performance of IS-Match is sufficient to deliver an interactive system and generate satisfactory results.

4.3 Sub-Matching Contours Clustering

The initial sub-matching pairs obtained in the previous section provide evidences of shape matches at local scales. To extract partial shape matches at larger scales, we need to accumulate these local evidences by grouping sub-matches into clusters. This requires the definition of a feature descriptor for each sub-matching pair and a distance metric in the feature space. Thus we characterize a sub-matching pair using the corresponding 2D rigid transformation $\mathbf{T} = (d_x, d_y, \theta)$ and define the distance metric between two rigid transformations as the weighted norm $\|\mathbf{T}_i - \mathbf{T}_j\|^2 = (d_x^i - d_x^j)^2 + (d_y^i - d_y^j)^2 + \beta(\theta^i - \theta^j)^2$. The weight β is used to adjust the relative influence of the translation and rotation components [31]. In our experimental setting, we set the weight so that a rotation by 180 degree corresponds to a displacement of half the bounding box diagonal of C_a. We apply the non-parametric mean shift clustering algorithm to the corresponding data points with kernel and bandwidth

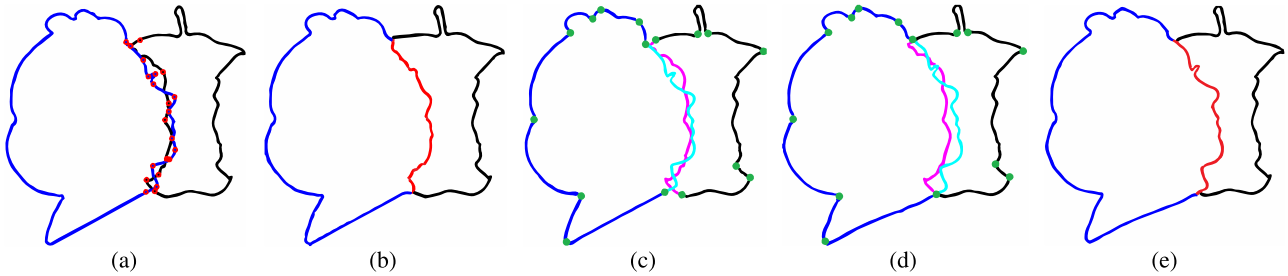

Fig. 6. Adaptive contour deformation pipeline. (a) Two matched partial contours with contour points shown in red dots. (b) A naive approach to generate a compound contour by stitching up each pair of matching points. Note that the shapes of both matching contours are smoothed out. (c) The configuration of control points (green dots) used in constrained curve deformation. (d) Two matching contours are fused at end control points, while the remaining contour points are deformed via the rigid transformations derived from control points. (e) The compound contour is generated by selecting the deformed partial contour with prominent convexity cues (i.e., Snow white's profile) as a common boundary shared by two objects.

functions as suggested in [32] to obtain clusters of sub-matches with similar rigid transformations (see Fig. 4c).

4.4 Optimal Partial Contour Matching

Once we have clusters of sub-matching contours, our goal in this section is to analyze and integrate constituent matching contour points to obtain an optimal partial contour matching for each cluster. This can be drawn as a weighted bipartite graph matching where the goal is to find a one-to-one mapping, i.e., a permutation π, among all pairs of matching points in the cluster that minimizes the objective function:

$$H(\pi) = \sum_i [\omega_s f_s(a_i, b_{\pi(i)}) + \omega_c f_c(a_i, b_{\pi(i)}) + \omega_d f_d(a_i, b_{\pi(i)}, \tilde{\mathbf{T}}) - f_q(a_i, b_{\pi(i)})]. \quad (8)$$

For each pair of matching points $\{a_i, b_{\pi(i)}\}$, i.e., an edge in the graph, the cost function f_s, similar to equation (2), returns the average shape similarity cost of all associated sub-matching contours that contain the pair. f_c and f_d measure the convex matching cost and shape deformation cost, respectively. Note that we use the average rigid transformation $\tilde{\mathbf{T}}$ of all sub-matching contours within the cluster to evaluate the shape deformation cost. The function f_q computes the normalized frequency of the pair among all pairs of the matching points in the cluster. The minimum weighted bipartite matching problem is solved using the Hungarian algorithm [33], and the optimal permutation is denoted as π^*. Nevertheless, π^* is not guaranteed to be order-preserving and may create crossed matching as shown in Fig. 5a. Hence, we further refine π^* by finding a longest increasing subsequence using dynamic programming and removing those crossed matching pairs (see Fig. 5b). Then we resolve the permutation problem for those unpaired contour points. This process iterates until we obtain a sequence of order-preserving matching points (see Fig. 5c). The system then ranks the optimal partial contour matching retrieved from clusters via the combined cost function in Equation (7) and selects the top five results as candidate partial shape matching pairs (see Fig. 4e).

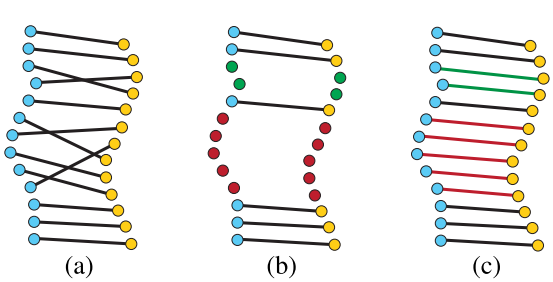

Fig. 5. (a) The minimum weighted bipartite graph where the matching points are not order-preserved. The problem is solved by (b) finding the longest increasing subsequence, removing the crossed matching pairs, and (c) resolving the permutation for the unpaired contour points.

5 Adaptive Contour Deformation

Given a candidate matching pair $\{c_a, c_b, \pi, \mathbf{T}\}$ suggested by our system, the next step is to combine two matched object contours into a compound contour. For this purpose, the system first maps C_a onto C_b using the rigid transformation $\mathbf{T}$. We denote the transformed C_a and corresponding partial contour c_a as $\tilde{C}_a$ and $\tilde{c}_a$, respectively. A naive approach to generate a compound contour would be to use the bijective function π and move both matching points $\{\tilde{a}_i, b_{\pi(i)}\}$ to the same point in the middle of line connecting two points. Obviously, this simple approach may dramatically damage the shapes of matching contours (see Fig. 6b). We solve the problem using a constrained rigid curve deformation to fuse two matching contours at both ends and selecting the side with most salient convexity features as the common boundary.

Specifically, we employ an adaption of the state-of-the-art MLS image deformation [34] to rigid deformation for 2D curves [35] to achieve smooth deformation. This deformation mechanism is driven by a set of control points, which are represented by the vertices of an approximated polyline of a contour in our case. The key idea is to find new positions of control points and apply the derived rigid transformations to contours such that (i) the deformed matching points are spatially coincident with each other; and (ii) the deformed matching contours should resemble the original shape (i.e., convexity cues). Note that the former criterion represents a hard constraint to stitch up matching contours precisely at each pair of matching points and is difficult to comply under the rigid transformation. We relax it by considering only the end points of matching contours and introduce a soft constraint that favors proximity of the remaining matching points under the rigid transformation. In this way we modify the configuration of control points by adding extra control points at both ends of matching contours and removing those ones within the matching contours (see Fig. 6c). We denote the end control points of $\tilde{c}_a$ and c_b as

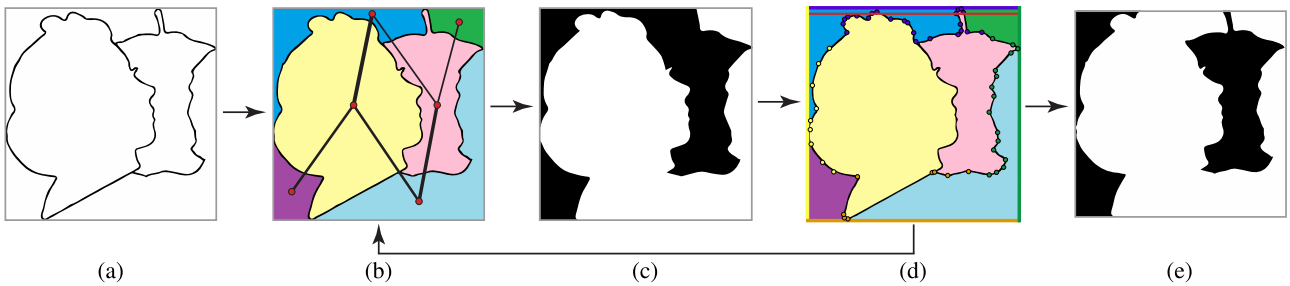

Fig. 8. EM-like iteration for optimizing the image cropping and binarization. (a) Using the bounding rectangle of two objects as an initial cropping window. (b) The constructed adjacency graph with the thickness of edges being proportional to their relative weights. (c) Computing an optimal binary color assignment based on the graph shown in (b). (d) Moving the top edge downward to improve the objective function in Equation (10). The edge and its associated vertices are color coded similarly. The steps (b)-(d) iterate until convergence. (e) The optimized result.

$\{\tilde{a}_j, \tilde{a}_k\}$ and $\{b_{\pi(j)}, b_{\pi(k)}\}$, respectively. The problem of fusing two matching contours at both ends is formulated as:

$$\{l_a^*, l_b^*\} = \arg\min_{\{l_a, l_b\}} \Big[\sum_{\forall a_i \in c_a} (\|l_a(\tilde{a}_i) - l_b(b_{\pi(i)})\|^2 + |\alpha_a(a_i) - \alpha_a(l_a(\tilde{a}_i))|^2 + |\alpha_b(b_{\pi(i)}) - \alpha_b(l_b(b_{\pi(i)}))|^2) \Big], \quad \text{s.t. } l_a(\tilde{a}_i) = l_b(b_{\pi(i)}), \text{for } i \in \{j, k\}, \tag{9}$$

where l_a and l_b are rigid transformations derived respectively from the displacement of control points $\{\tilde{a}_j, \tilde{a}_k\}$ and $\{b_{\pi(j)}, b_{\pi(k)}\}$. Equation (9) is a constrained nonlinear optimization problem, which is computationally expensive to solve. To reduce the search space, we further simplify the problem by refining the hard constraint to

$$l_a(\tilde{a}_i) = l_b(b_{\pi(i)}) = (1.0 - t_i)\tilde{a}_i + t_i b_{\pi(i)}, \text{ for } t_i \in [0.0, 1.0], i \in \{j, k\},$$

which constrains the fused position to lie on the line connecting two matching contour points. Thus Equation (9) can be solved efficiently using conventional direction set methods such as Powell's conjugate direction method [36]. Fig. 6d shows an example. Once we have two matching contours that are fused at both ends, the shared boundary between deformed contours $l_a^*(\tilde{C}_a)$ and $l_b^*(C_b)$ is simply determined by choosing among $l_a^*(\tilde{c}_a)$ and $l_b^*(c_b)$ the one with larger average magnitude of convexity cues (see Fig. 6e).

6 Image Cropping and Binarization

Given the the compound object contour denoted as $C' = C'_a \cup C'_b$, the last step is to compute an optimal window frame enclosing the compound contour and binary color assignment of pixels to composite the final binary image. In a naive approach, one can simply crop the image using the bounding rectangle of a particular object, and fill the interior of contour with black (or white) while treating the rest of regions as a white (or black) background. As shown in Fig. 7, although such a simple approach perfectly keeps the shape of one object, it largely sacrifices the shape of the other; it can only be recognized at the shared boundary. To address the problem, we propose a joint optimization that simultaneously computes image cropping and binarization to maximize the completeness of both object contours as illustrated in Fig. 8.

Fig. 7. The naive approach for rendering the final image. (Left) The input compound contour. The results generated using the bounding rectangles of Snow White and an apple core are show on the middle and right, respectively.

Let us denote a cropping window as $\mathbf{w} = (x, y, W, H)$, representing a window with dimensions $W \times H$ that is placed at the integer location (x, y) in the image. According to the boundary of $\mathbf{w}$, C'_a and C'_b, the system divides the image into disjoint regions $R(\mathbf{w}) = \{r_1, \ldots, r_{n(\mathbf{w})}\}$ by extracting connected components in image domain using a flood fill algorithm. We denote the regions enclosed by C'_a and C'_b as r_a and r_b, respectively. Next we construct an adjacency graph $G = (V, E)$ with each vertex in V corresponds to a region. An edge $e_{i,j}$ is added to E when two regions r_i and r_j adjoin each other. The edge weight $l_{i,j}$ encodes the length of shared boundary between r_i and r_j. Fig. 8b shows such a graph. Our goal is to compute a cropping window $\mathbf{w}$ and a binary color assignment of regions, $B(\mathbf{w}) = \{b_1, \ldots, b_{n(\mathbf{w})} | b_i \in 0, 255\}$, that maximize the equation:

$$\{\mathbf{w}^*, B^*\} = \arg\max_{\{\mathbf{w}, B\}} \left[\frac{1}{\|C'_a\|} \sum_{\substack{e^a_{ij} \in E \\ b_i \neq b_j}} l_{i,j} + \frac{1}{\|C'_b\|} \sum_{\substack{e^b_{ij} \in E \\ b_i \neq b_j}} l_{i,j} \right], \tag{10}$$

with $e^a_{i,j}$ and $e^b_{i,j}$ denoting the edges that are incident respectively to r_a and r_b. Equation (10) measures the proportion of object contours retained in the final binary image. Note that the structure of the adjacency graph varies with the parameters of the cropping window. Hence it is computationally expensive and infeasible to solve Equation (10) using a brute-force algorithm. We employ an EM-like iteration [37] to efficiently obtain a local maximum.

We first initialize the cropping window $\mathbf{w}$ using a bounding rectangle of $C'_a \cup C'_b$ (see Fig. 8a). In the E step, we optimize the binary color assignment B by fixing the parameters of $\mathbf{w}$. This is equivalent to finding a maximum weighted spanning tree of the adjacency graph G. We use Prim's algorithm, which starts from a tree with two vertices $\{r_a, r_b\}$ and initial color assignment $\{b_a = 255, b_b = 0\}$. The tree is augmented greedily by adding an edge (r_i, r_j) with maximal weight such that r_j is a vertex adjacent to the tree

and the insertion does not introduce any cycle. Then we assign r_j the opposite color of r_i. Fig. 8c shows an example of optimized binary color assignment.

The M step aims at adjusting the parameters of **w** to improve the objective function. However, it is intractable using a gradient search in the parametric space because different configurations of **w** may correspond to the same adjacency graph G. Thus, we adopt a heuristic approach to identify a subset of valid configurations that will potentially improve the objective function (i.e., changing the structure of G). We first approximate the outer contour of $C'_a \cup C'_b$ using a polyline of which the vertices are classified into four sets based on their proximity to four edges of **w** as shown in Fig. 8d. The M step is formulated as moving one of the four edges of **w** to one of the associated vertices. Thus, we experimentally test every possible movement by translating the edge either vertically or horizontally to each associated vertex and run the E step. We choose among all the movements the one that best improves the objective function and update **w** accordingly. The process iterates until no more improvement can be found. Fig. 8e shows an example of optimized result.

7 User Controls and Application

User controls. Although the proposed algorithm runs automatically, our system currently supports users the following intuitive controls to assist the creation process:

- *Region of interest.* The user is able to specify the region of interest for an input object through a marquee selection tool, while the system utilizes the selected partial contour to guide the shape matching process.
- *Ranking re-ordering.* In addition to the top ranked partial shape match, the system simultaneously shows the user the four other alternatives sorted by their shape matching costs. The user then selects the one she prefers and proceeds the creation process.
- *Cropping control.* The user can override the optimized cropping window by specifying a new one via a drag-and-drop mouse interface, while the system automatically updates the binary color assignment in the background.

Automatic search by ranking. In addition to above user controls, we also develop a simple search mechanism to automatically retrieve matching candidates from a database. Given an object and a target database, the system first exhaustively searches the best matching result with respect to every object in the database. The results are then ranked using the combined shape matching cost in Equation (7), and the system suggests and displays top 5 ones (see supplementary video, available online, at 2:20).

We believe such an interactive system will not only facilitate creating ambiguous figure-ground images for amateurs, but also benefit skillful artists to initiate their art pieces. We refer the reader to the supplementary video, available online, and executable program to experience such a creation process.

8 Results and Evaluation

We have tested our system on a dataset with 183 clip arts comprised of a wide variety of shapes, including humans, animals, plants, insects, man-made objects, etc. Using our system, 80 results are created with or without user intervention. Please refer to the supplementary material, available online, for a complete gallery. Some examples can be found in Fig. 9. Note that in addition to results composed of two objects, our system is also capable of combining multiple objects to produce aesthetically pleasing results (see Figs. 9a, 9b, 9c, 9d, 9e, 9f, 9g). Moreover, only a few images (see Figs. 9a, 9b, 9c, 9d, 9e, 9f, 9g, 9l, 9s, 9t) are generated with simple user assistance to specify a region of interest for partial shape matching. In general, creating ambiguous figure-ground images using our system is easy and intuitive, involving only a few clicks to go through the three-stage pipeline (see supplementary video, available online). In the following sections, we conducted several experiments to quantitively and qualitatively evaluate our system.

TABLE 1
Timing Performance of Our System

	partial shape matching	contour deformation	cropping and binarization	overall
avg.	0.7	0.020	0.06	0.78
std. dev.	0.4	0.006	0.03	0.4

The completion time, measured in seconds, is averaged over all results.

8.1 Timing Performance

Table 1 details the average running times of our system for generating all results. As we can see, the proposed algorithm is fast and takes less than a second on average to generate a result. The major computational burden lies in the partial shape matching process and is proportional to the complexity of the input contours.

8.2 Shape Matching Metric Evaluation

The shape matching metric defined in Equation (7) combines five energy terms to evaluate the quality of the partial shape matching. To evaluate the effectiveness of individual energy terms, we conducted a small experiment that compares the visual quality of a few results generated with or without enabling a particular energy term in the partial shape matching stage. Fig. 10 shows five examples, corresponding to the side-by-side comparisons of each energy term. More comparisons can be found in the supplementary material, available online. We can tell from the results that each energy term indeed plays a role in capturing important features for matching partial contours to render promising ambiguous figure-ground images.

8.3 Performance of Partial Shape Matching

To validate the effectiveness of proposed content-aware partial shape matching algorithm, we compare the visual quality of our results with those generated by the state-of-the-art partial shape matching algorithm. Specifically, we prepared 53 pairs of images, each of which contains one image from our results while the other is generated by adopting the method of Donoser et al. [27] in the partial shape matching stage to retrieve a partial contour matching with maximum shape similarity (see supplementary material, available online). We conducted a user study, in which

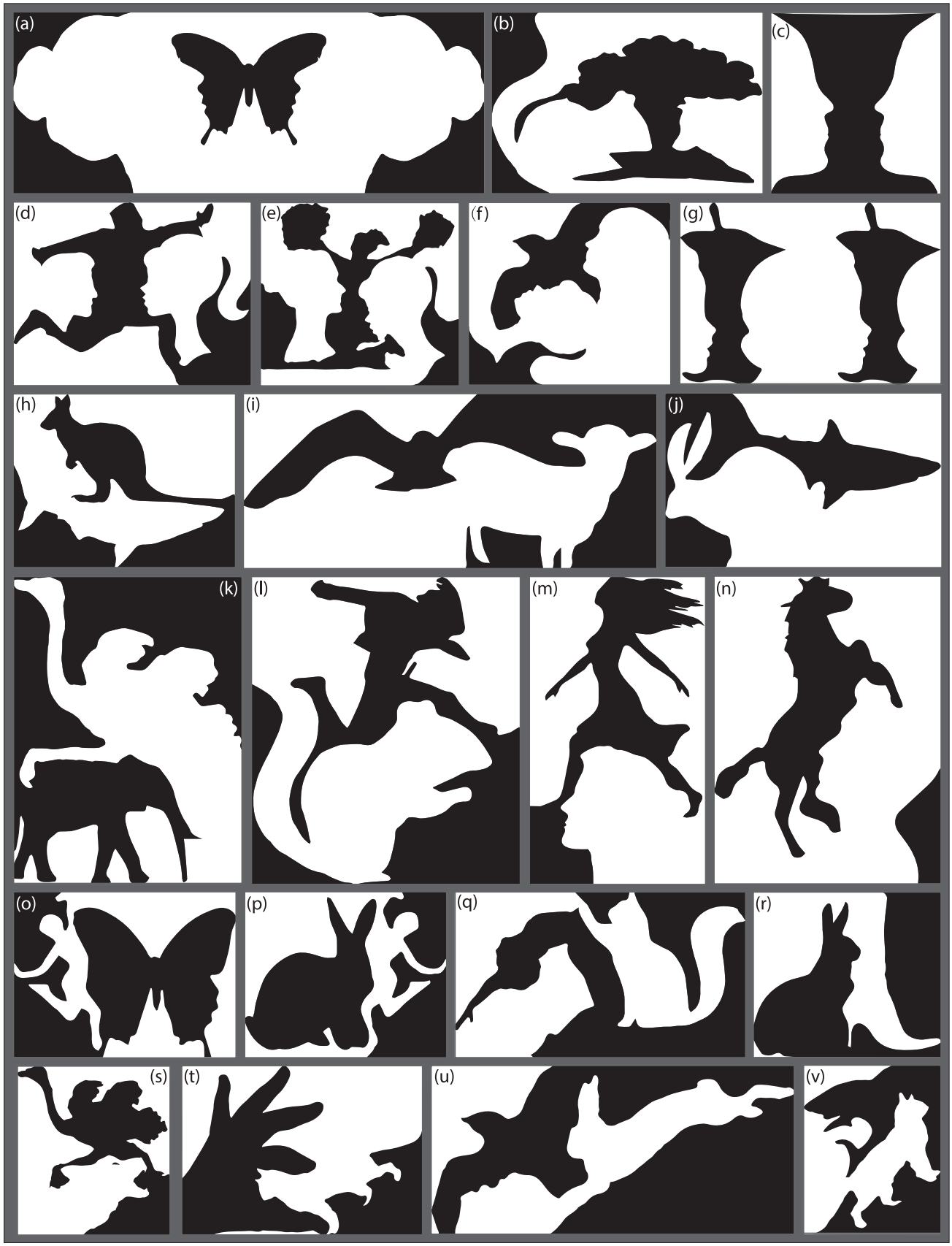

Fig. 9. Twelve ambiguous figure-ground images generated using our system with or without user intervention. (a)-(g) show four image compositions using more than two objects, while (h)-(v) are eight results composed of two objects. Our system is efficient and takes less than a second to generate these visually appealing results either automatically or with simple user assistance to specify the region of interest for shape matching ((a)-(g),(l),(s),(t)).

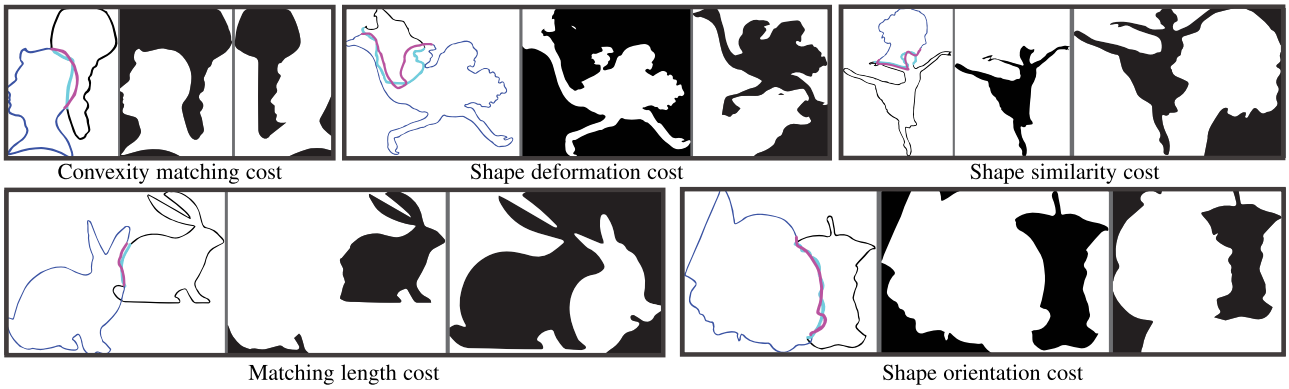

Fig. 10. Evaluating the influence of individual energy terms in Equation (7) on the quality of results. In each example, we show (Left) the partial matching contours retrieved by the system and (Middle) the corresponding result without enabling a particular energy term as labeled below. (Right) The original result.

six participants were recruited to view all 53 images and asked to pick among each pair the one that best interprets the ambiguous figure-ground perception. Note that each participant was first instructed on the nature of ambiguous figure-ground perception using the Rubin's Face–Vase image. In each display, the images were shown in a side-by-side random arrangement. Not surprisingly, our results won about 94 percent of the vote, indicating that the conventional shape matching, that only takes into account shape similarity, can not guarantee a promising result. An example can be found in Figs. 11a, 11b where the conventional shape matching is likely to partially match the shapeless contours. We also looked into the images where the preference is reversed and found analogous results generated by both approaches as shown in Figs. 11c, 11d.

8.4 Ranking Evaluation

We mentioned in Section 4.4 that the system ranks all retrieved partial shape matching pairs according to the cost function in Equation (7), and suggests users only the top five scoring results. We hypothesize that the quality of resultant ambiguous figure-ground images is related to the rank of partial shape matching. Since the ultimate judgement of image quality is by humans, we conducted a user study to verify the hypothesis. We recruited five participants with prior knowledge about ambiguous figure-ground perception to collaboratively look through 800 examples. Each example was comprised of two objects randomly picked from our dataset and five results were generated according to five candidates suggested by the system. Then 160 displays, each containing five results from an example arranged in random order, were shown to a participant. In each display, the participant is asked to vote for the one out of five results she/he found most visually engaging and best interpretation of the ambiguous figure-ground perception. Fig. 12a shows the voting results, which indicate a trend that participants' preferences tend to favor images with a higher ranking in partial shape matching, and thus verifies our hypothesis.

8.5 Figure-Ground Ambiguity Test

A good ambiguous figure-ground image should achieve a delicate balance in figural competition between two contiguous regions and present viewers with the visual phenomena of perceiving either the white or black region as foreground while treating the other as background at any moment. In order to evaluate the effectiveness of images created by our system, we conducted a user study involving nine participants with normal vision to view a sequence of 37 images. The image sequence was comprised of five target images from our results and organized to have five repeated occurrences of each target image with three normal object images filling in between image repetitions. We followed the procedure similar

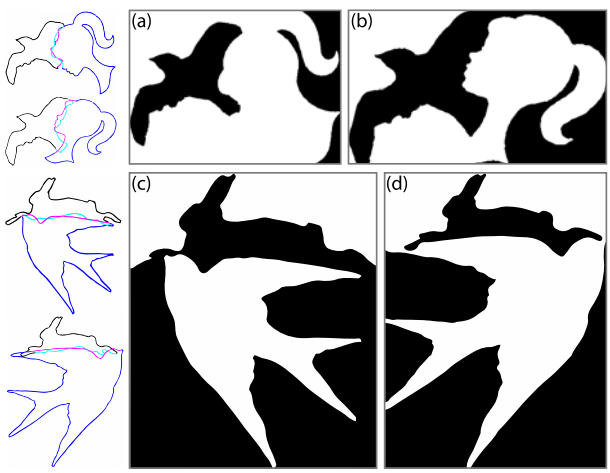

Fig. 11. Two examples in the comparison with conventional partial shape matching. (a,c) The results generated by Donoser et al. [27]. (b,d) Our results. The retrieved partial matching contours are shown on the left.

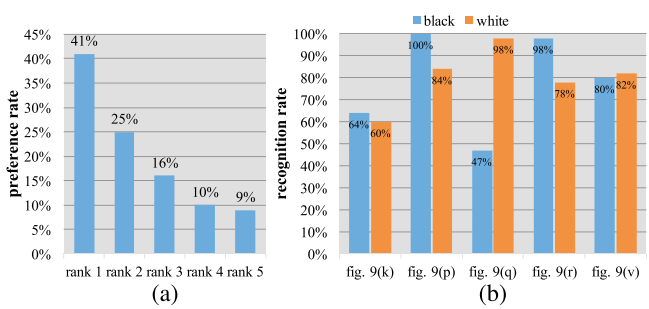

Fig. 12. User study statistics. (a) Preference rate and (b) recognition rate of generated ambiguous figure-ground images as observed in course of user study (see Section 8).

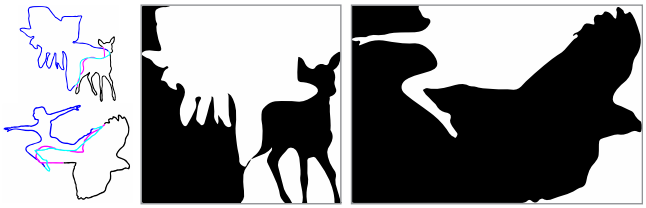

Fig. 13. Failed examples. (a) Severe shape degeneration (e.g., deer's rear leg) caused by contour deformation. (b) Both the right half of the human and lower half of the bird are missing after the image binarization.

to [5] to capture which objects (i.e., black/white regions) are perceived as figures by participants at an instant. Specifically, each image was displayed for 300 ms followed by a blank display, then participants were asked to recognize and name the object(s) they saw. The study began by instructing participants using three example trials, and we recorded the answer(s) given by participants for each target image. Fig. 12b shows the recognition rates of the two objects in each target image. The numbers indicate that regions in most of examples (see Figs. 9k, 9p, 9r, 9v) are equally likely to be seen as foreground figures under an instant display, which agrees with the expected visual phenomena. Though a mediocre result (see Fig. 9q) is observed, which might possibly be attributed to the unfamiliar posture of human figure (e.g., gymnastic pose), we still obtain a reasonable recognition rate close to 50 percent.

8.6 Limitations

Limitations of our algorithm are as follows: (i) The partial shape matching algorithm still inherits the setting of conventional approaches and might fail to find good partial contour matching between complex shapes. For instance, the IS-Match will return a large number of short and diverse sub-matching contours that can not be effectively aggregated into clusters. (ii) Since we assume mild contour deformation to generate the compound contour, it will sometimes cause severe shape degeneration in the cases that demand substantial contour deformation (see Fig. 13a). (iii) A good partial shape matching result does not always guarantee high quality ambiguous figure-ground images due to the restriction of binary representation in which a tradeoff of keeping shapes between objects has to be made as shown in Fig. 13b.

9 Conclusion and Future Work

Ambiguous figure-ground images are fascinating and entertaining to both ordinary people and artists as they present viewers an interesting visual phenomena of perceiving multiple interpretations from a single black and white image. We present an automatic algorithm to generate such images from two arbitrary objects and develop an interactive system with several assistant toolkits to facilitate the creation process. Experimental study indicates that our system not only significantly reduces the tedious manual efforts during the creation to only a few clicks, but also produces results that are proved by human viewers to be effective and visually engaging. With the aid of our system, amateurs can enjoy the efficient exploration of creating ambiguous figure-ground images, while skilled artists can use it for initial design of their artworks to reduce their production time.

Several interesting future works lie ahead. First, we can further improve the robustness of the system by employing the partial shape matching algorithm by Riemenschneider et al. [28] to support input objects with open contours. Second, we plan to study a more sophisticated shape deformation to improve the quality of our results, particularly for articulated figures. However, a tradeoff between time complexity and quality needs to be carefully evaluated. Our shape matching metric considers only local geometric features, while artists would frequently utilize the global shape features such as symmetry in their designs to enhance the aesthetic feeling. Thus, it will be worth exploring the incorporation of symmetry detection [38] into our framework. Moreover, the metric is also unaware of semantic features (e.g., eyes, noses, etc), and therefore can not take into account the relative importance of such features in both shape matching and deformation stages. While automatic detection could be difficult, we plan to utilize user scribbles to prescribe different weights for different regions. Finally, the efficiency of our algorithm enables the possibility of creating a massive number of results, which will potentially benefit studies in cognitive psychology via providing diverse visual stimulus.

Acknowledgments

The authors thank the anonymous reviewers for their invaluable comments and suggestions; Charles Morace for proofreading. The project was supported in part by the Ministry of Science and Technology of Taiwan (102-2221-E-007-055-MY3, 103-2221-E-007-065-MY3, 104-2218-E-004-003, and 104-2221-E-006-044-MY3).

References

[1] V. Bruce, P. R. Green, and M. A. Georgeson, *Visual Perception: Physiology, Psychology, and Ecology.*, Psychology Press, Hove, United Kingdom, 2003.
[2] P. K. Kienker, T. J. Sejnowski, G. E. Hinton, and L. E. Schumacher, "Separating figure from ground with a parallel network," *Perception*, vol. 15, no. 2, pp. 197–216, 1986.
[3] M. A. Peterson and B. S. Gibson, "Object recognition contributions to figure-ground organization: Operations on outlines and subjective contours," *Perception Psychophys.*, vol. 56, no. 5, pp. 551–564, 1994.
[4] M. A. Peterson and E. Skow, "Inhibitory competition between shape properties in figure-ground perception," *J. Exp. Psychol.: Human Perception Perform.*, vol. 34, no. 2, p. 251, 2008.
[5] M. A. Peterson and E. Salvagio, "Inhibitory competition in figure-ground perception: Context and convexity," *J. Vis.*, vol. 8, no. 16, p. 4, 2008.
[6] M. A. Peterson, "Low-level and high-level contributions to figure-ground organization," *Oxford Handbook Perceptual Org.*, Oxford University Press, Oxford, 2014.
[7] G. Kanizsa and W. Gerbino, "Convexity and symmetry in figure-ground organization," *Vis. Artifact*, pp. 25–32, 1976.
[8] M. A. Peterson, E. M. Harvey, and H. J. Weidenbacher, "Shape recognition contributions to figure-ground reversal: Which route counts?" *J. Exp. Psychol.: Human Perception Perform.*, vol. 17, no. 4, p. 1075, 1991.
[9] M. A. Peterson, "Object perception," *Blackwell Handbook of Sensation and Perception*, Hoboken, NJ, USA: Wiley, pp. 168–203, 2001.
[10] (2010). Pinterest [Online]. Available: http://www.pinterest.com/soates80/figure-ground/
[11] E. Rubin, "Figure and ground," *Readings Perception*, pp. 194–203, 1958.

[12] M.-T. Chi, T.-Y. Lee, Y. Qu, and T.-T. Wong, "Self-animating images: illusory motion using repeated asymmetric patterns," *ACM Trans. Graph.*, vol. 27, no. 3, p. 62, 2008.
[13] N. J. Mitra and M. Pauly, "Shadow art," *ACM Trans. Graph.*, vol. 28, no. 5, pp. 156:1–156:7, 2009.
[14] N. J. Mitra, H.-K. Chu, T.-Y. Lee, L. Wolf, H. Yeshurun, and D. Cohen-Or, "Emerging images," *ACM Trans. Graph.*, vol. 28, no. 5, pp. 163:1–163:8, 2009.
[15] J.-C. Yoon, I.-K. Lee, and H. Kang, "A hidden-picture puzzles generator," *Comput. Graphics Forum*, vol. 27, no. 7, pp. 1869–1877, 2008.
[16] H.-K. Chu, W.-H. Hsu, N. J. Mitra, D. Cohen-Or, T.-T. Wong, and T.-Y. Lee, "Camouflage images," *ACM Trans. Graph.*, vol. 29, pp. 51:1–51:8, 2010.
[17] Q. Tong, S.-H. Zhang, S.-M. Hu, and R. R. Martin, "Hidden images," in *Proc. ACM SIGGRAPH/Eurograph. Symp. Non-Photorealistic Animation Rendering*, 2011, pp. 27–34.
[18] C. S. Kaplan and D. H. Salesin, "Escherization," in *Proc. 27th Annu. Conf. Comput. Graphics Interactive Techn.*, 2000, pp. 499–510.
[19] R. Gal, O. Sorkine, T. Popa, A. Sheffer, and D. Cohen-Or, "3D collage: Expressive non-realistic modeling," in *Proc. ACM SIGGRAPH/Eurograph. Symp. Non-Photorealistic Animation Rendering*, 2007, p. 14.
[20] H. Huang, L. Zhang, and H.-C. Zhang, "Arcimboldo-like collage using internet images," *ACM Trans. Graph.*, vol. 30, no. 6, pp. 155:1–155:8, Dec. 2011.
[21] Q. Tong, S. hai Zhang, R. R. Martin, and P. L. Rosin, "Nested images," in *Proc. Asian Conf. Des. Digital Eng.*, 2011, pp. 445–450.
[22] R. C. Veltkamp and M. Hagedoorn, *State of the Art in Shape Matching*. New York, NY, USA: Springer, 2001.
[23] T. F. Cootes, C. J. Taylor, D. H. Cooper, and J. Graham, "Active shape models-their training and application," *Comput. Vis. Image Understanding*, vol. 61, no. 1, pp. 38–59, 1995.
[24] L. J. Latecki, R. Lakamper, and T. Eckhardt, "Shape descriptors for non-rigid shapes with a single closed contour," in *Proc. IEEE Conf. Comput. Vis. Pattern Recog.*, 2000, vol. 1, pp. 424–429.
[25] S. Belongie, J. Malik, and J. Puzicha, "Shape matching and object recognition using shape contexts," *IEEE Trans. Pattern Anal. Mach. Intell.*, vol. 24, no. 4, pp. 509–522, Apr. 2002.
[26] A. C. Berg, T. L. Berg, and J. Malik, "Shape matching and object recognition using low distortion correspondences," in *Proc. IEEE Conf. Comput. Vis. Pattern Recog.*, 2005, vol. 1, pp. 26–33.
[27] M. Donoser, H. Riemenschneider, and H. Bischof, "Efficient partial shape matching of outer contours," in *Proc. 9th Asian Conf. Comput. Vis.*, 2010, pp. 281–292.
[28] H. Riemenschneider, M. Donoser, and H. Bischof, "Using partial edge contour matches for efficient object category localization," in *Proc. Eur. Conf. Comput. Vis.*, 2010, pp. 29–42.
[29] J. Xu and C. S. Kaplan, "Artistic thresholding," in *Proc. ACM SIGGRAPH/Eurograph. Symp. Non-Photorealistic Animation Rendering*, 2008, pp. 39–47.
[30] D. H. Douglas and T. K. Peucker, "Algorithms for the reduction of the number of points required to represent a digitized line or its caricature," *Cartographica*, vol. 10, no. 2, pp. 112–122, 1973.
[31] N. M. Amato, O. B. Bayazit, L. K. Dale, C. Jones, and D. Vallejo, "Choosing good distance metrics and local planners for probabilistic roadmap methods," *IEEE Trans. Robot. Autom.*, vol. 16, no. 4, pp. 442–447, Aug. 2000.
[32] D. Comaniciu and P. Meer, "Mean shift: A robust approach toward feature space analysis," *IEEE Trans. Pattern Anal. Mach. Intell.*, vol. 24, no. 5, pp. 603–619, May 2002.
[33] C. H. Papadimitriou and K. Steiglitz, *Combinatorial Optimization: Algorithms and Complexity*. Englewood Cliffs, NJ, USA: Prentice-Hall, 1982.
[34] S. Schaefer, T. McPhail, and J. Warren, "Image deformation using moving least squares," *ACM Trans. Graph.*, vol. 25, no. 3, pp. 533–540, Jul. 2006.
[35] (2013). Shape manipulation with moving least squares for curves [Online]. Available: http://www.morethantechnical.com/2013/01/05/shape-manipulation-with-moving-least-squares-for-curves-w-code/
[36] W. H. Press, S. A. Teukolsky, W. T. Vetterling, and B. P. Flannery, *Numerical Recipes 3rd Edition: The Art of Scientific Computing*, 3rd ed. Cambridge, U.K.: Cambridge Univ. Press, 2007.
[37] A. P. Dempster, N. M. Laird, and D. B. Rubin, "Maximum likelihood from incomplete data via the em algorithm," *J. Roy. Statist. Soc., Series B*, vol. 39, no. 1, pp. 1–38, 1977.
[38] N. J. Mitra, L. Guibas, and M. Pauly, "Partial and approximate symmetry detection for 3d geometry," *ACM Trans. Graph.*, vol. 25, no. 3, pp. 560–568, 2006.

Ying-Miao Kuo received the BS degree in computer science from National Tsing Hua University, Taiwan, in 2013. Now, She working toward the PhD degree at the Department of Computer Science, National Tsing Hua University. Her research interests include computer graphics, non-photorealistic rendering, and recreational graphics.

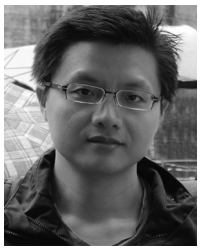

Hung-Kuo Chu received the BS and PhD degrees from the Department of Computer Science and Information Engineering, National Cheng-Kung University. He is an assistant professor at the Department of Computer Science, National Tsing Hua University. His research interests focus on shape understanding, smart manipulation, perception-based rendering, recreational graphics, and human computer interaction.

Ming-Te Chi received the MS and PhD degrees from the Department of Computer Science and Information Engineering, National Cheng-Kung University, Taiwan, in 2003 and 2008, respectively. He is currently an associate professor of the Department of Computer Science, National Chengchi University. His research interests include computer graphics, non-photorealistic rendering, and information visualization.

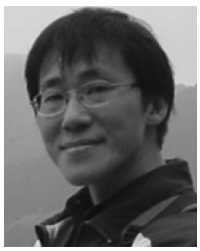

Ruen-Rone Lee received the PhD degree in computer science from National Tsing Hua University, Taiwan, in June 1994. From 1994 to 2010, he worked in several IC design companies for graphics hardware and software development. Later, from 2010 to 2015, he was an associate researcher with the Department of Computer Science, National Tsing Hua University. He is currently a deputy director in the Information and Communications Research Laboratories, Industrial Technology Research Institute, Hsinchu, Taiwan. His research interests include computer graphics, non-photorealistic rendering, and graphics hardware architecture design. He is a member of the IEEE Computer Society and a member of the ACM SIGGRAPH.

Tong-Yee Lee received the PhD degree in computer engineering from Washington State University, Pullman, in May 1995. He is currently a chair professor in the Department of Computer Science and Information Engineering, National Cheng-Kung University, Tainan, Taiwan, ROC. He leads the Computer Graphics Group, Visual System Laboratory, National Cheng-Kung University (http://graphics.csie.ncku.edu.tw/). His current research interests include computer graphics, non-photorealistic rendering, medical visualization, virtual reality, and media resizing. He is a senior member of the IEEE and the member of the ACM.